

Motion compensation using a suctioning stabilizer for intravital microscopy

Claudio Vinegoni,^{1,2,†,*} Sungon Lee,^{1,3,†} Rostic Gorbatov¹ and Ralph Weissleder^{1,2}

¹Center for System Biology; Massachusetts General Hospital and Harvard Medical School; Boston MA, USA; ²Center for Molecular Imaging Research; Massachusetts General Hospital and Harvard Medical School; Charlestown, MA USA; ³Interaction and Robotics Research Center; Korea Institute of Science and Technology; Seoul, Korea

[†]These authors contributed equally to this work.

Keywords: intravital microscopy, motion compensation, optical microscopy, in vivo imaging, cardiac imaging

Motion artifacts continue to present a major challenge to single cell imaging in cardiothoracic organs such as the beating heart, blood vessels or lung. In this study, we present a new water-immersion suctioning stabilizer that enables minimally invasive intravital fluorescence microscopy using water-based stick objectives. The stabilizer works by reducing major motion excursions and can be used in conjunction with both prospective or retrospective gating approaches. We show that the new approach offers cellular resolution in the beating murine heart without perturbing normal physiology. In addition, because this technique allows multiple areas to be easily probed, it offers the opportunity for wide area coverage at high resolution.

Introduction

Intravital fluorescence microscopy continues to be increasingly used as a research tool to decipher biology in complex environments. The ability to provide cellular and subcellular resolution images of organs in live animals has enabled major advances in diverse fields such as tumor biology, immunology and neurobiology.¹⁻⁶ Despite advances in optics and instrumentation, biological motion (particularly respiratory and cardiac motion) places severe constraints on the resolution, imaging time and coverage achievable; furthermore, it limits our capability for imaging many visceral organs. To date, a variety of organ-specific stabilizing “holders” have been designed, each of which have been shown to reduce motion sufficiently as to allow imaging of the kidneys, arteries, brain, lungs as well as more recently, hearts.⁷⁻¹⁸ In these studies, a common strategy involves exteriorizing and compressing the organ with a coverslip, essentially squeezing the organ to reduce motion. While this solution is reasonable for organs that are easily mobilized and which show only low levels of native motion (e.g., liver, pancreas and transplanted hearts),^{6,18} this approach is less well suited to organs such as the heart, which can move more than 500 μm during a single cardiac cycle. In addition, the coverslip method often requires fairly strong compression, which can impair normal physiology. In the heart, for example, such mechanical constraints can distort the reproducibility of the cardiac motion, which makes it impossible to combine the method with other gating techniques. A possible alternative strategy to the coverslip method would be to perform ultrafast, multipoint confocal imaging, which would

have the effect of “freezing” motion.¹⁹ In practice, however, such high speed imaging techniques have been hampered by the fact that cardiac motion is subject to six degrees of freedom in space (x, y, z and three angular movements in the chest cavity), which often change in a non-reproducible way. Each single frame would therefore correspond to a different randomly imaged optical section within the tissue.

A recently proposed methodology¹² consisted in using a rigid motion stabilizer in combination with an algorithm for acquisition during advanced cardiopulmonary gating. While this technique was demonstrated to provide exquisite spatial resolution (subnuclear) it does not offer the possibility to easily sample different parts of an organ in particular when accessing areas deep within the abdominal or thoracic cavity. Another solution to the problem of motion artifacts has involved using negative pressure (vacuum suctioning) to image the lungs during respiratory motion.¹³⁻¹⁷ Based on this technique, we herein present a similar negative pressure method for imaging the beating murine heart. The purpose of the suctioning holder in this study is to make the cardiac motion range more reproducible so that it can be more easily gated. The holder also satisfies the following two requirements: (1) unlike positive pressure methods, the holder does not restrict natural blood flow through the myocardium. Rather, it uses a slight negative pressure to maintain the imaged area within a reproducible motion trajectory, all while keeping the heart in its original position within the chest cavity. (2) Because the stabilizer holder is very small, it can access internal organs through a minimal incision in the chest or abdominal cavity. By also accommodating a stick-type water immersion micro-objective with a short

*Correspondence to: Claudio Vinegoni; Email: vinegoni@mgh.harvard.edu
Submitted: 09/16/2012; Revised: 11/23/2012; Accepted: 11/27/2012
<http://dx.doi.org/10.4161/intv.23017>

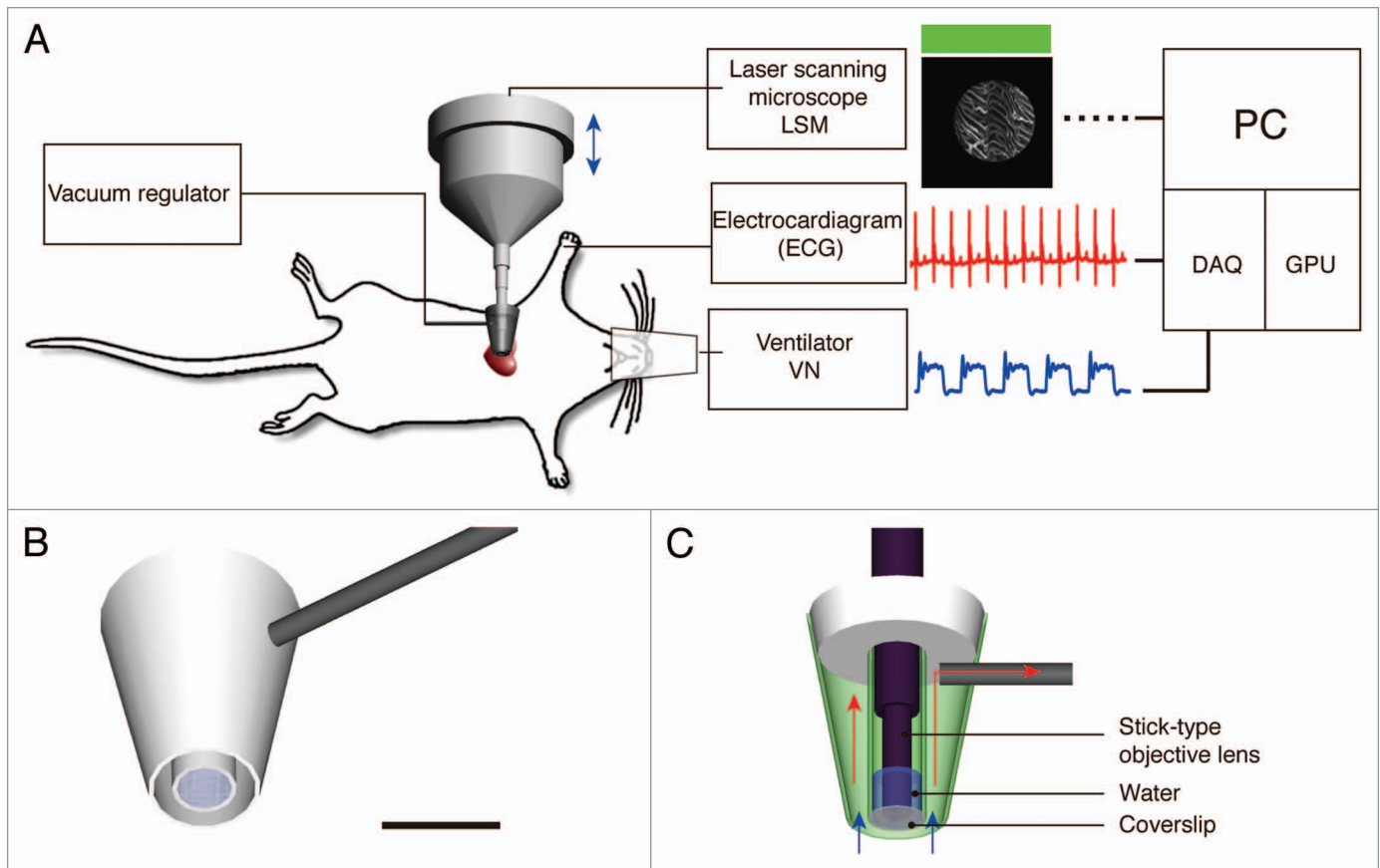


Figure 1. Experimental setup. (A) The heart imaging system consists of a custom-made vacuum-based heart stabilizer (for allocating different water immersion stick-type objective lenses), an electrocardiogram (ECG) recorder and amplifier, a small animal ventilator, a laser scanning microscope (LSM), acquisition signal electronics and an elaborating unit. The murine heart is held in contact with the stabilizer via a gentle negative pressure. During imaging, ECG signals, lung airway pressure signals and the microscope scan timing signals are recorded for image reconstruction via retrospective gating. (B) A three-dimensional schematic model of the custom-made heart stabilizer. The stabilizer is connected to a vacuum regulator through a 1 mm-diameter metal conduit (gray). Scale bar 5 mm. (C) Side section view of B with a stick-type objective lens. Arrows indicate the direction of the suction flow. The outer chamber of the stabilizer is under negative pressure and provides the vacuum, which gently holds the heart tissue in place. The internal chamber is maintained at standard pressure and is filled with water for index matching of the objective lens. A coverslip glued at the end of the second chamber prevents water from leaking out. The myocardium is in direct contact with the coverslip.

probing length, specifically developed for intravital microscopy, the stabilizer can be easily positioned on the organ's surface; this offers the possibility of sampling multiple areas during a single imaging session. In this report, we present some of the first high resolution intravital images of the beating murine heart.

Results

Stabilizer design and implementation. The miniaturized suctioning stabilizer consists of two distinct chambers, one internal chamber and one external chamber. The diameter of the external chamber is 4.5 mm, whereas the internal chamber provides a 2 mm-diameter viewing window through which a water immersion-based micro-lens objective is used to image the tissue (Fig. 1). The internal chamber is also filled with water for index matching of the objective lenses and is sealed with a thin coverslip (Fig. 1B and C). Vacuum is maintained in the external chamber through the use of a 1 mm-diameter conduit that connects the external chamber to a vacuum regulator. It is

important to maintain vacuum only in the external chamber in order to ensure that the immersing water is not suctioned away. The possibility to maintain water in the inner chamber is crucial for being able to utilize water immersion objectives and for taking advantage of index matching conditions. Once the vacuum is established in the external chamber, cardiac movements can be controlled in a reproducible way, which is an essential condition when working with gating imaging modalities. The suctioning pressure levels are controlled by two vacuum regulators, which are serially mounted and connected to the external chamber via the conduit. For fine positioning (planar and angular) and for other final adjustments prior to imaging, the stabilizer is attached to a 6 degrees of freedom micromanipulator. By varying the amount of pressure, the holder can then be released and reapplied multiple times to sample different areas of the imaged organ.

Mouse preparation. Imaging was performed using a customized Olympus FV1000-MPE laser scanning microscopy system in confocal mode. This system is based on an upright BX61-WI microscope. During imaging, mice were ventilated and all

physiological parameters, including electrocardiogram (ECG) measurements, were recorded. The chest wall was held open using a retractor, and the stabilization holder was then inserted into the chest cavity. To facilitate suctioning and adhesion of the heart to the coverslip, and to ensure that the exposed heart remained undamaged, sterile phosphate buffered saline (PBS) was used periodically to moisten the surface of the heart. The miniaturized stabilizer was then positioned and a negative pressure of $\sim 50\text{--}75$ mm Hg was applied. The pressure value was arbitrarily chosen in order to provide sufficient contact with the heart and achieve a specific motion compensated resolution. Different values of pressure can be chosen depending on the geometry of the holder and the degree of stabilization pursued. The water-immersion based objective was then lowered into the water-filled internal chamber and positioned in contact with the coverslip. The stabilizer thus does not compress the heart nor block its motion during contractions. Rather, it allows the heart to move with reproducible motion that can be easily gated. We used two miniaturized high performance objectives (see also Material and Methods for more details). With their high numerical apertures and water immersion optics, these objectives guarantee superior performance both in terms of resolution as well as aberration correction. They are thus the optimal choice for intravital deep tissue imaging, particularly with regards to gradient index (GRIN) lenses or fiber bundles.

Image acquisitions and reconstructions were performed using a triggering or retrospective gating approach (see also Material and Methods for more details). This strategy enabled images with high signal-to-noise ratios (high integration time per pixel) as well as large pixel numbers to be obtained. For cases where fast dynamic events need to be observed (i.e., cells moving within blood vessels), a fast free-running acquisition modality can be implemented in combination with the stabilizer (Vid. S1).

Imaging the beating heart. Figure 2 shows example images of cardiac microvasculature, acquired either with the suctioning stabilizer (Fig. 2C) or with a compressive coverslip (Fig. 2A). In both cases, consecutive frames triggered at a specific timepoint within the cardio and respiratory cycles were acquired. As can be clearly seen, images taken using the compressive coverslip method are incomplete and each image is different from the next. In contrast, images taken with the stabilizer method are complete and entirely reproducible during subsequent acquisitions. To quantify stabilization, we determined the Pearson's coefficient of the images by calculating the two-dimensional correlation between frames, both without (Fig. 2B) and with (Fig. 2D) the proposed stabilizer. Our findings showed that whereas the Pearson's coefficient between images taken with the stabilizer (red line, Fig. 2D) was ~ 0.8 , indicating that consecutive images triggered at a specific timepoint within the cardio and respiratory cycle were very similar to one another, the coefficient between images acquired without the holder was much lower (~ 0.25).

Although the boundary constraints induced by the stabilizer reduced the overall motion components, the acquired images still contained motion artifacts due to myocardial contraction and respiration. From vessel movements, we estimated that the remaining motion was approximately less than $10\ \mu\text{m}$ in all

dimensions. While this remaining component is small compared with the natural excursions of the exposed heart ($500\ \mu\text{m}$), it is still significant enough to result in motion artifacts, particularly in high magnification images. Fortunately, these residual motion artifacts can be easily removed by image reconstruction using either retrospective or prospective approaches. These acquisition modalities are frequently used in cardiac MRI and in electrocardiographically-gated coronary computed tomographic angiography where motion components and exposure times are of critical importance. During prospective imaging, acquisitions are triggered at well-defined moments in time with respect to a physiological signal (appearance of a QRS complex in the ECG signal, for example). While we could have chosen such a modality we opted also for a more general retrospective approach because not all commercial imaging systems offer the opportunity to be fast triggered. In this modality images are continuously acquired while physiological parameters are monitored. At the appearance of a specific electrophysiological signal during the cardiac cycle, data are extracted from the acquired images and used to build a final "reconstructed image" (Fig. 3).

Electrocardiogram (ECG) traces, lung airway pressure, and microscope scanning signals from the microscope were then each recorded during imaging via an analog-to-digital acquisition interface. Reconstruction tests determined that the optimal time-gating window for minimizing motion artifacts was located at the end of the diastolic phase in the left ventricle (time window W2) and within the stationary phase at the end of expiration in the respiratory cycle (time window W1). Image patches from multiple images that corresponded to this specific gating period (W3) at the intersection between W1 and W2, were then collected and overlaid to generate motion-free image reconstructions. Here, W3 was set equal to $43\ \text{ms}$ and 25 image patches were collected for a final high-resolution reconstruction (Fig. 3). The acquired image patches were very stable and reproducible presenting a high cross-correlation over time, when the acquisition was synchronized with the ECG. For instance, black dots in Figure 2D indicate the cross-correlation between image patches acquired within the same temporal stabilized window W3 as defined in Figure 3, but belonging to different images triggered on the same SQR complex within the ECG. The high value of cross-correlation (~ 1) indicates the high degree of stabilization and reproducibility obtained through the use of the stabilizer and the gated imaging approach.

To determine the extent of cardiac motion during imaging, fluorescein isothiocyanate (FITC)-labeled fluorescent beads were injected into live mice. Beads trapped within the myocardial capillaries subsequently served as stable fiducial markers (Fig. 4A). In Figure 4B, the position of one bead is shown across several frames following application of the stabilizer. When no gating is considered the position of the bead is reproducible within 6 microns. When instead data within the temporally stabilized window (W3) were considered, the variation in the bead's position was greatly reduced (area bound by the red circle), and thus the image resolution significantly increased ($2\ \mu\text{m}$). A comparison between an image obtained using our reconstruction method and an image acquired post-mortem of the same area demonstrated the effectiveness of the proposed stabilization

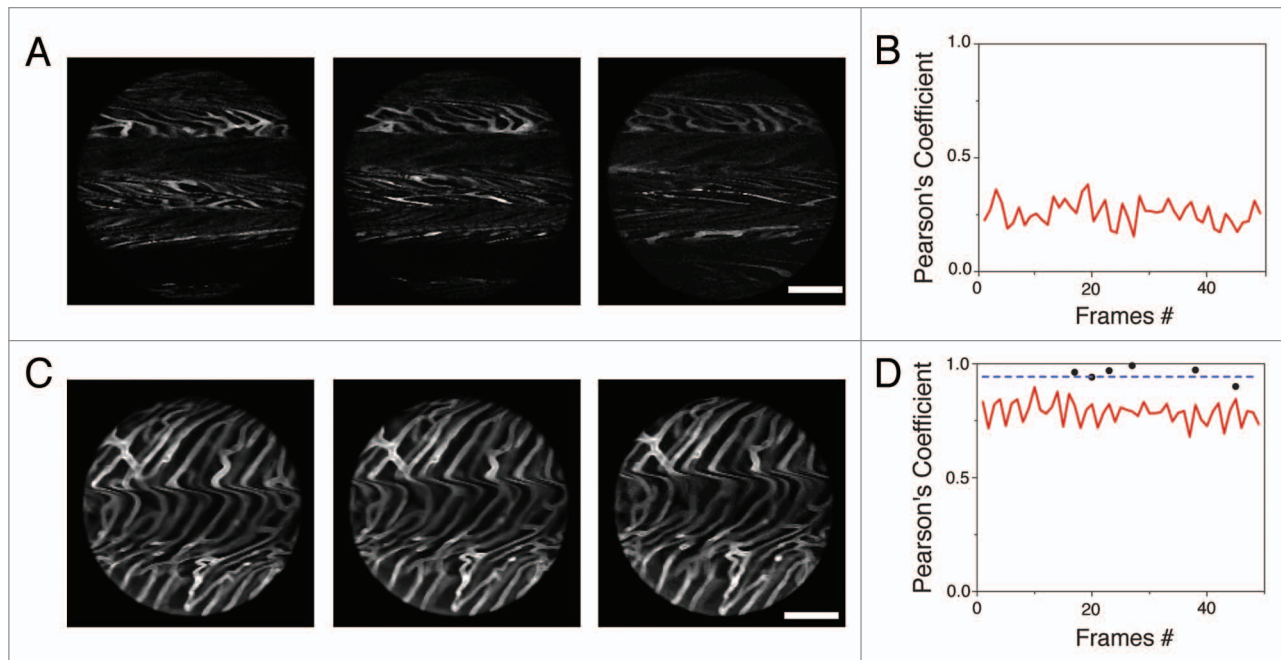


Figure 2. Images of cardiac microvasculature acquired without (A) or with (C) the proposed stabilizer (triggered at the beginning of the “temporal stabilized window”; see Fig. 3). The cross correlation (Pearson’s Coefficient) was calculated on the whole image frames acquired both without (B) or with (D) the stabilizer (0.25 and 0.8 respectively). Black dots instead indicate the correlation between image patches, within different frames, collected at the temporal stabilized window (W3; Fig. 3). Due to the reduced motion activity during this phase of the cardiac cycle, the value of cross correlation is increasingly higher for this portion of images (~1).

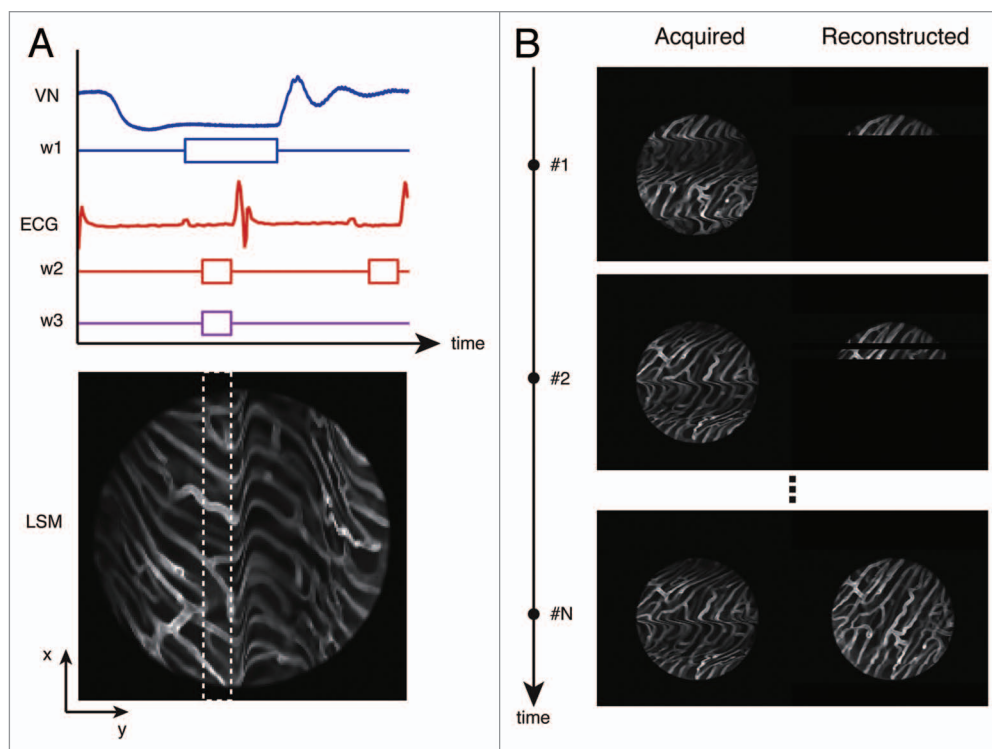


Figure 3. Top left, a timing diagram for image acquisition. VN, lung airway pressure trace; W1, the gating window centered at the end of the expiration phase; ECG, electro-cardiogram trace recording; W2, the gating window at the end of the diastolic phase; W3, the temporally stabilized window. Bottom left, acquired images exhibit motion artifacts due to heart beat and respiration. Within the raw image, an undistorted area was observed at the point where end-diastole coincided with end-expiration; data were collected from the area (patch) bound by the white dashed box within the distortion-free temporally stabilized window (W3). Right, by collecting sequential images through retrospective gating or prospective triggering (images on the left), images of undistorted areas (right) could be obtained and reconstructed to generate a final artifact-free image (bottom right image).

technique (Fig. 4C and D). For Figure 4C, W3 was equal to 32 ms and 50 image patches were collected. To test if the stabilizer affected the normal physiology of the heart we monitored several physiologic parameters during typical anesthesia such as heart rate, respiratory rate, temperature and hydration. ECG signals acquired at different times before, and during intravital imaging sessions (Fig. 5) do not present any noticeable differences indicating normal electrical heart activity. Tissue integrity was not compromised during and after imaging and no damage was present in the microvascular network on the surface of the heart in direct contact with the stabilizer (Fig. 5E and F).

Discussion

In this report, we describe the design and testing of a new water-immersion suctioning stabilizer for minimally invasive intravital microscopy of orthotopic organs. The stabilizer can be used in conjunction with prospective and retrospective gating methods, and is applicable to other organs where motion artifacts prohibit acquisition of high-resolution images. The method does not affect normal physiology of the heart nor does it cause any damage during imaging. By gently applying and releasing the suctioning holder via pressure control, the technique allows rapid repositioning, which in turn offers the possibility for larger areas of interest to be imaged without motion artifacts. While both prospective or retrospective acquisition modalities are more suited for obtaining high resolution images with high SNR, continuous high frame rate acquisition can be also implemented in order to image dynamic events such as monitoring leukocytes trafficking in the heart microvasculature (Vid. S1).

Materials and Methods

Microscope objectives. Two different objectives were used in combination with our stabilizer (6× IV-OB13F67W20, 20× IV-OB13F20W20; Olympus).²⁰ Both objectives have a small diameter (1.3 mm), a working distance of 200 μm (with numerical apertures of 0.5 and 0.14 respectively), a short probing length (approximately 1 cm), and a field of view of 200 and 670 μm respectively. The transmission of these objectives ranges from 62% to 78% throughout the visible and near-infrared parts of the spectrum.

Mouse preparation. During imaging, mice were anesthetized, intubated and ventilated via an animal ventilator (Harvard Apparatus INSPIRA ASV 55-7058), which delivered 2% isoflurane supplemented with 2L/minute oxygen. Mice were placed in a supine position on a heating pad, which maintained their temperature at 37°C, and a thoracotomy was then performed. During surgery and imaging, several physiological parameters were monitored including respiratory rate, temperature, hydration, blood pressure and oxygenation, etc. To facilitate imaging and to stain capillary vessels, Griffonia simplicifolia lectin was injected intravenously via tail vein 10 min before imaging.

Image processing. Image acquisitions and reconstructions were performed using a prospective triggering or retrospective gating approach (Fig. 3). A Discrete Wavelet Transform (DWT)

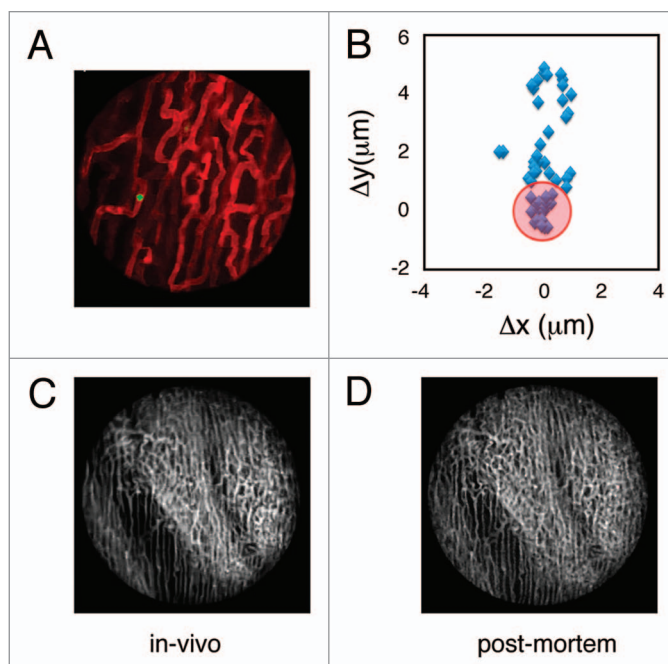


Figure 4. (A) A reconstructed stabilized image of the cardiac microvasculature stained with lectin (red). FITC-labeled beads (5 μm diameter; green) were injected into the live mouse prior to imaging. Beads trapped within the vasculature were subsequently used as fiducial markers to quantify tissue displacement caused by motion. Images were acquired with a 6x MicroProbe objective (Olympus, IV-OB13F67W20). (B) The position of a single bead (blue diamonds) was determined across several frames following application of the stabilizer. When the bead's position was determined within the temporal stabilized window (W3), the amount of displacement was greatly reduced (variations in the bead's position are indicated by the red circle). A comparison between in vivo reconstructions (C) and post-mortem imaging (D) demonstrates the effectiveness of the proposed method.

was used to extract QRS complexes, which correspond to a portion of deflections on the electrocardiogram representing the ventricular depolarization, and P waves (detected in real-time) from the ECG signals.²¹ An adjustable gating time window (W2; typically 15–40 ms), positioned after the P wave and just before the QRS complex, and coinciding with the end-diastole of the left ventricle, was determined within each ECG cycle. The occurrence of this interval within the cardiac cycle, in combination with a specific interval at the end-expiration phase (W1), was defined as the “temporally stabilized window” (W3); this was the point at which images were acquired. This selection process was repeated in real-time for all acquired images until an artifact-free stabilized image was achieved. Fast dynamic events can be recorded in real time without post-processing but only relying on the stabilizer motion compensation.

Disclosure of Potential Conflicts of Interest

No potential conflicts of interest were disclosed.

Acknowledgments

This project was funded in part by Federal funds from the National Heart, Lung, and Blood Institute, National Institutes

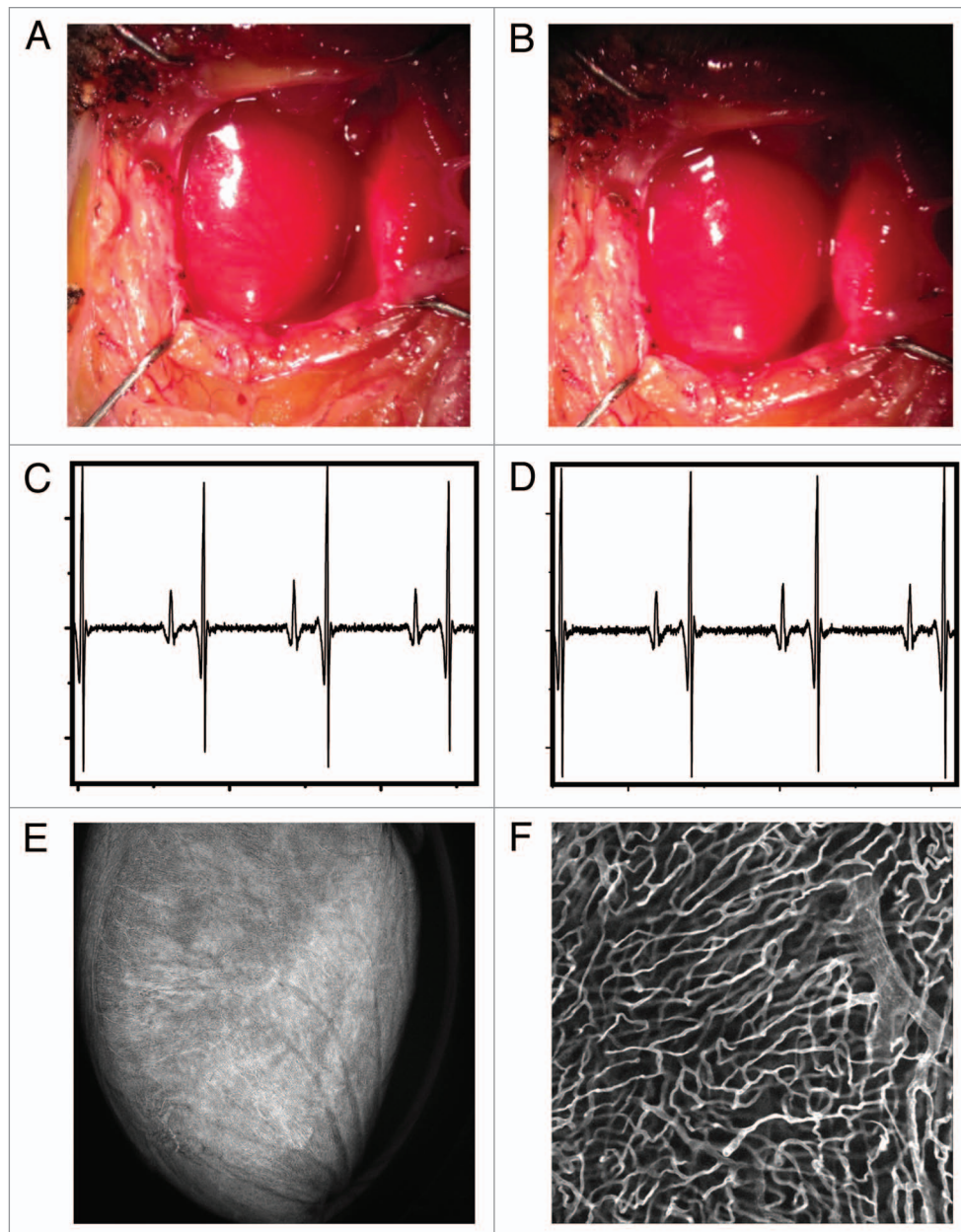


Figure 5. White light image of the heart before (A) and after (B) application of the stabilization holder. After removal of the stabilizer no damage is evident from the images. ECG signals acquired at different times before the intravital imaging session (C) and after the stabilizer has been positioned on the heart (D). No noticeable differences are present in the ECG signals, indicating normal electrical heart activity during the imaging session. (E and F) In order to demonstrate that the stabilizer did not alter the capillary structures, the mouse was injected intravenously with 50 μ L of a 10 nM solution of Griffonia simplicifolia-I lectin (Ex 550 nm, Em 575 nm), which binds specifically to the mouse endothelial cells staining the capillaries. After removal of the stabilizer the mouse was euthanized and the heart immediately imaged. No damage was present in the microvascular network on the surface of the heart at both the macroscopic (E) and microscopic (F) level. (F) Was acquired in confocal mode at a depth of ca. 50 microns in the point of contact between the stabilizer and the heart.

of Health, Department of Health and Human Services (under Contract No. HHSN26820100004xC) and from the Institute of Biomedical Engineering (under R01EB006432).

Supplemental Materials

Supplemental materials may be found here:
www.landesbioscience.com/journals/intv/article/23017

References

1. Pittet MJ, Weissleder R. Intravital imaging. *Cell* 2011; 147:983-91; PMID:22118457; <http://dx.doi.org/10.1016/j.cell.2011.11.004>.
2. Sumen C, Mempel TR, Mazo IB, von Andrian UH. Intravital microscopy: visualizing immunity in context. *Immunity* 2004; 21:315-29; PMID:15357943; [http://dx.doi.org/10.1016/S1074-7613\(04\)00237-7](http://dx.doi.org/10.1016/S1074-7613(04)00237-7).
3. Weigert R, Sramkova M, Parente L, Amornphimoltham P, Masedunskas A. Intravital microscopy: a novel tool to study cell biology in living animals. *Histochem Cell Biol* 2010; 133:481-91; PMID:20372919; <http://dx.doi.org/10.1007/s00418-010-0692-z>.
4. Ritsma L, Ponsioen B, van Rheenen J. Intravital imaging of cell signaling in mice. *IntraVital* 2012; 1:1-8.
5. Bullen A. Microscopic imaging techniques for drug discovery. *Nat Rev Drug Discov* 2008; 7:54-67; PMID:18079755; <http://dx.doi.org/10.1038/nrd2446>.
6. Condeelis J, Weissleder R. In vivo imaging in cancer. *Cold Spring Harb Perspect Biol* 2010; 2:a003848; PMID:20861158; <http://dx.doi.org/10.1101/cshperspect.a003848>.
7. Flusberg BA, Nimmerjahn A, Cocker ED, Mukamel EA, Barretto RP, Ko TH, et al. High-speed, miniaturized fluorescence microscopy in freely moving mice. *Nat Methods* 2008; 5:935-8; PMID:18836457; <http://dx.doi.org/10.1038/nmeth.1256>.
8. Megens RTA, Reitsma S, Prinzen L, oude Egbrink MG, Engels W, Leenders PJ, et al. In vivo high-resolution structural imaging of large arteries in small rodents using two-photon laser scanning microscopy. *J Biomed Opt* 2010; 15:011108; PMID:20210434; <http://dx.doi.org/10.1117/1.3281672>.
9. Lee S, Nakamura Y, Yamane K, Toujo T, Takahashi S, Tanikawa Y, et al. Image Stabilization for In Vivo Microscopy by High-Speed Visual Feedback Control. *IEEE Trans Robot* 2008; 24:45-54; <http://dx.doi.org/10.1109/TRO.2007.914847>.
10. Gioux S, Ashitate Y, Hutteman M, Frangioni JV. Motion-gated acquisition for in vivo optical imaging. *J Biomed Opt* 2009; 14:064038; PMID:20059276; <http://dx.doi.org/10.1117/1.3275473>.
11. Sandoval RM, Kennedy MD, Low PS, Molitoris BA. Uptake and trafficking of fluorescent conjugates of folic acid in intact kidney determined using intravital two-photon microscopy. *Am J Physiol Cell Physiol* 2004; 287:C517-26; PMID:15102609; <http://dx.doi.org/10.1152/ajpcell.00006.2004>.
12. Lee S, Vinegoni C, Feruglio PF, Fexon L, Gorbatov R, Pivoravov M, et al. Real-time in vivo imaging of the beating mouse heart at microscopic resolution. *Nat Commun* 2012; 3:1054; PMID:22968700; <http://dx.doi.org/10.1038/ncomms2060>.
13. Wagner WW Jr. Pulmonary microcirculatory observations in vivo under physiological conditions. *J Appl Physiol* 1969; 26:375-7; PMID:5773180.
14. Presson RG Jr., Brown MB, Fisher AJ, Sandoval RM, Dunn KW, Lorenz KS, et al. Two-photon imaging within the murine thorax without respiratory and cardiac motion artifact. *Am J Pathol* 2011; 179:75-82; PMID:21703395; <http://dx.doi.org/10.1016/j.ajpath.2011.03.048>.
15. Kuhnle GE, Leipfing FH, Goetz AE. Measurement of microhemodynamics in the ventilated rabbit lung by intravital fluorescence microscopy. *J Appl Physiol* 1993; 74:1462-71; PMID:8482691.
16. Kuebler WM, Parthasarathi K, Lindert J, Bhattacharya J. Real-time lung microscopy. *J Appl Physiol* 2007; 102:1255-64; PMID:17095639; <http://dx.doi.org/10.1152/japplphysiol.00786.2006>.
17. Looney MR, Thornton EE, Sen D, Lamm WJ, Glenn RW, Krummel MF. Stabilized imaging of immune surveillance in the mouse lung. *Nat Methods* 2011; 8:91-6; PMID:21151136; <http://dx.doi.org/10.1038/nmeth.1543>.
18. Li W, Nava RG, Bribriaco AC, Zinselmeyer BH, Spahn JH, Gelman AE, et al. Intravital 2-photon imaging of leukocyte trafficking in beating heart. *J Clin Invest* 2012; 122:2499-508; PMID:22706307; <http://dx.doi.org/10.1172/JCI62970>.
19. Liebling M, Forouhar AS, Gharib M, Fraser SE, Dickinson ME. Four-dimensional cardiac imaging in living embryos via postacquisition synchronization of nongated slice sequences. *J Biomed Opt* 2005; 10:054001; PMID:16292961; <http://dx.doi.org/10.1117/1.2061567>.
20. Alencar H, Mahmood U, Kawano Y, Hirata T, Weissleder R. Novel multiwavelength microscopic scanner for mouse imaging. *Neoplasia* 2005; 7:977-83; PMID:16331883; <http://dx.doi.org/10.1593/neo.05376>.
21. Li C, Zheng C, Tai C. Detection of ECG characteristic points using wavelet transforms. *IEEE Trans Biomed Eng* 1995; 42:21-8; PMID:7851927; <http://dx.doi.org/10.1109/10.362922>.